Available online at www.sciencedirect.com

ScienceDirect

Ceramics International 40 (2014) 1029–1035

CERAMICS INTERNATIONAL

www.elsevier.com/locate/ceramint

Novel akermanite-based bioceramics from preceramic polymers and oxide fillers

Enrico Bernardo[a,*], Jean-François Carlotti[a], Pedro Mendanha Dias[a], Laura Fiocco[a], Paolo Colombo[a,b], Laura Treccani[c], Ulrike Hess[c], Kurosch Rezwan[c]

[a]*Dipartimento di Ingegneria Industriale, University of Padova, Italy*
[b]*Department of Materials Science and Engineering, The Pennsylvania State University, USA*
[c]*Advanced Ceramics Group, Faculty of Production Engineering, University of Bremen, Germany*

Received 19 April 2013; received in revised form 6 June 2013; accepted 26 June 2013
Available online 2 July 2013

Abstract

Akermanite ($Ca_2MgSi_2O_7$) ceramics have been successfully prepared by a novel approach, consisting of the heat treatment of silicone resins embedding MgO and CaO precursors, in the form of micro- and nano-sized particles, that act as reactive fillers. Phase purity was promoted by the use of nano-sized particles or by secondary additives, such as sodium borate. The use of hydroxyapatite as additional filler allowed the fabrication of monoliths with good specific mechanical properties, although with a complex phase assemblage. Sodium borate, besides favoring the crystallization of the desired silicate, promoted a substantial and homogeneous foaming of polymer/filler mixtures, leading to akermanite foams possessing good compressive strength.

Keywords: B. Porosity; D. Silicate; E. Biomedical applications; Polymer-derived ceramics

1. Introduction

The $CaO–SiO_2$ system has been widely demonstrated to provide excellent biomaterials, in the form of glasses (bioglasses [1]), glass-ceramics (e.g. wollastonite–apatite glass-ceramics [2]) and polycrystalline ceramics (e.g. wollastonite polymorphs, di-calcium silicate etc. [3–5]). The investigations concerning the most recent bioceramics, however, have underlined the possible improvements in bone-like apatite-formation ability and bioactivity associated with the presence of additional oxides [6].

MgO has been always recognized as a key secondary oxide in bioceramics, being already present in the formulation for wollastonite-based glass-ceramics [2] and some bioglasses [1]. Another interesting contribution of this oxide concerns the formation of new phases, i.e. Ca–Mg silicates, in polycrystalline ceramics, which are the object of a growing interest by researchers [7–12].

Akermanite, $Ca_2MgSi_2O_7$ (or $2CaO \cdot MgO \cdot 2SiO_2$), is the most reported bioactive Ca–Mg silicate, together with diopside ($CaMgSi_2O_6$, or $CaO \cdot MgO \cdot 2SiO_2$). Compared to those based on wollastonite, ceramics bases on Ca–Mg silicates are generally stronger and are subjected to a slower degradation in body fluids; in addition, the ionic products may stimulate cell proliferation [9].

In the present work, akermanite ceramics are fabricated following a novel approach, based on silicone resins, filled with micro- or nano-sized oxide particles [13]. According to this method, the fillers directly react with the product of oxidative decomposition of the resins, consisting of amorphous silica, possessing a particularly defective network and consequently prone to very favorable reaction kinetics. A distinctive feature of preceramic polymers, including silicones, is that a component may be shaped in the polymeric form using plastic forming technologies and later converted into a ceramic; applied to silicones embedding CaO precursors (mainly $CaCO_3$) this concept has already led to several examples of wollastonite cellular ceramics, including 3D scaffolds [14]. In the case of akermanite, we will show firstly the conditions

*Corresponding author.
E-mail address: enrico.bernardo@unipd.it (E. Bernardo).

0272-8842/$ - see front matter © 2013 Elsevier Ltd and Techna Group S.r.l. All rights reserved.
http://dx.doi.org/10.1016/j.ceramint.2013.06.100

for the synthesis of the desired phase in condition of high purity and relatively low processing temperature and secondly the fabrication of highly porous components through the use of fillers able to perform a double role, i.e. they both react with the silicone residue to give the desired crystalline phases and act as foaming agents.

2. Materials and Methods

2.1. Materials

Two commercially available silicones, MK and H62C (Wacker-Chemie GmbH, Munich, Germany) were used as silica sources. MK is a powder, while H62C is a highly viscous liquid. The polymers were first dissolved in isopropanol and then mixed with micro- and nano-sized fillers, consisting of CaO and MgO precursors (primary fillers). CaO was provided by $CaCO_3$, in form of microparticles (< 10 μm, Sigma Aldrich, Gillingham, UK) or nanoparticles (PlasmaChem, Berlin, Germany, 90 nm), whereas MgO came from $Mg(OH)_2$ microparticles (< 10 μm, Industrie Bitossi, Vinci, Italy) or MgO nanoparticles (Inframat Advanced Materials, Manchester, CT, USA, 30 nm). Selected formulations comprised also hydroxyapatite (later referred to as HAp; P260 S, Plasma Biotal Ltd, Tideswell, UK, $d_{50} = 3$ μm) and borax (sodium borate decahydrate, $Na_2B_4O_7 \cdot 10H_2O$, Normapur Prolabo, France) microparticles. The balance among the most important constituents (silicones/CaO precursor/MgO precursor) followed the stoichiometric SiO_2/CaO/MgO molar proportions of akermanite (i.e. SiO_2/CaO/MgO = 2/2/1). Isopropanol was used in an amount of 20 ml for every 10 g of starting materials.

The mixing was performed under magnetic stirring, followed by ultrasonication for 10 min, which allowed to obtain stable and homogeneous dispersions, later cast in large glass containers and left to dry overnight at 80 °C.

2.2. Preparation of monoliths and foams

Monoliths were prepared using both polymers as silica source. More precisely, 50 wt% of SiO_2 was due to MK, 50 wt% to H62C; given the relative silica yield (0.84 for MK, 0.58 for H62C), the polymers were used in the weight proportion MK/H62C = 2/3. This solution for silica precursors was chosen after preliminary experiments concerning other silicates and alumino-silicates, such as wollastonite and cordierite [14,15]. Besides CaO and MgO precursors, some samples featured HAp as additional filler, in an amount ranging from 25 to 75 wt%. After drying at 80 °C in a glass container, the silicone/filler mixtures were heated at 200 °C (in order to favor the cross-linking of H62C, in analogy with previous experiences [15]), for 1 h, and then manually ground into fine powders by pestle and mortar. The powders were cold-pressed in a cylindrical steel die applying a pressure of 40 MPa for 2 min, without using any binder. Disc specimens with a diameter of 20 mm and thickness of approximately 1 mm were obtained and heat treated at 900–1100 °C for 1 h; the heating rate was 2 °C/min. For a selected formulation, the powders were pressed into a tile with dimensions of approximately 50 mm × 35 mm × 4 mm, by using a bigger die. After ceramization, the tile was cut into small beams of approximately 43 mm × 3 mm × 4 mm, later polished and chamfered, up to a 5 μm finish, by using diamond tools.

Foams were prepared by using only the H62C polymer, to which $Mg(OH)_2$ micro-particles, $CaCO_3$ micro- or nano-sized particles, and borax (5 and 15 wt% of the theoretical ceramic yield of the other components) were added. The use of H62C as the only silica source was aimed at maximizing the rheological behavior of the mixtures (in turn due to the fact that H62C is liquid at room temperature) [15]. After first drying at 80 °C, the H62C-based mixtures were in the form of thick pastes, later manually transferred into Al molds, where they were subjected to a treatment at 350 °C in air (direct insertion of samples in oven), for 30 min, which enabled to stabilize the bubbles caused by water release (from Mg hydroxide and borax). During the treatment, complete crosslinking of the preceramic precursors was also achieved. This treatment replaced the cross-linking cycle at 200 °C, previously applied to mixtures based on both MK and H62C. After removal from the Al molds, samples were fired at 1100 °C for 1 h in air (2 °C/min heating rate). Cylindrical samples, with diameter of 10 mm and height of 7–8 mm, were obtained from the fired foams, by manual polishing (with diamond tools).

Table 1
Summary of conditions for sample preparation.

Type	Silica precursor	Primary fillers (CaO and MgO precursors)	Secondary filler	Firing temperature (°C)	Expected crystal phases
Akermanite monoliths	MK/H62C	Micro-$CaCO_3$, Micro-$Mg(OH)_2$	None	900 1000	Akermanite
		Nano-$CaCO_3$, Nano-MgO		1100	
Akermanite/HAp composite monoliths	MK/H62C	Nano-$CaCO_3$, Nano-MgO	HAp (25–75 wt%)*	900 1100	Akermanite+HAp
Akermanite foams	H62C	Nano-$CaCO_3$ Micro-$Mg(OH)_2$	None	1100	Akermanite
			Borax (5–15 wt%)*		
		Micro-$CaCO_3$, Micro-$Mg(OH)_2$	Borax (5 wt%)*		

*Amounts referred to the theoretical ceramic yield of the silicone/primary fillers mixtures.

Table 1 summarizes the conditions for the preparation of samples, in both monolithic and cellular form.

2.3. Characterization

The density of discs and foams was determined geometrically and by weighing using a digital balance. The true density of the various samples was measured by means of a gas pycnometer (Micromeritics AccuPyc 1330, Norcross, GA), operating with He gas on samples in powdered form. Microstructural characterizations were performed by optical stereomicroscopy and scanning electron microscopy (FEI Quanta 200 ESEM, Eindhoven, The Netherlands) equipped with EDS.

The crystalline phase identification was performed by means of X-ray diffraction (XRD; Bruker AXS D8 Advance, Bruker, Germany), supported by data from PDF-2 database (ICDD-International Centre for Diffraction Data, Newtown Square, PA) and Match! program package (Crystal Impact GbR, Bonn, Germany).

The elastic modulus of akermanite/HAp composites was determined by subjecting the previously mentioned small beams to non-destructive dynamic resonance testing (Grindosonic, Leuven, Belgium). The bending strength of monolithic samples and the crushing strength of foams were measured at room temperature, by means of an Instron 1121 UTM (Instron Danvers, MA) operating with a cross-head speed of 1 mm/min. Bending tests were conducted in the 4-point configuration (40 mm outer span, 20 mm inner span). Each data point represents the average value of 5–10 individual tests.

3. Results and discussion

3.1. Synthesis of akermanite ceramics

Fig. 1 confirms the possibility to obtain akermanite ceramics exploiting the reactions between the ceramic residue from silicones and fillers. Considering the absence of an evident amorphous halo in all patterns, the total degree of crystallization was reputed to be remarkable already after the heat treatment at 900 °C. However, the yield of the desired silicate was strongly affected by the processing temperature and the size of the fillers. More precisely, as already found in previous investigations on wollastonite [13], the use of nano-sized particle fillers led to the formation of akermanite (PDF#87-0047) already at 900 °C, while a higher processing temperature was required when using micro-sized fillers of the same composition. Samples fired at 1000 °C did not show any significant difference with respect to the ones fired at 900 °C in terms of crystalline phase assemblage and overall peak intensity. At 1100 °C, akermanite was the main crystal phase in all samples, but the sample from micro-sized fillers contained more impurities (see the relative height of characteristic peaks), in the form of secondary silicates, such as wollastonite (β-$CaSiO_3$, PDF#84-0655) and merwinite ($Ca_3MgSi_2O_8$ i.e. $3CaO \cdot MgO \cdot 2SiO_2$, PDF#35-0591). The sample from micro-sized fillers also contained traces of unreacted MgO (periclase, PDF#87-0653). From the semiquantitative X-ray diffraction analysis provided by the Match! program package, we can say that the final phase assemblage at 1100 °C for

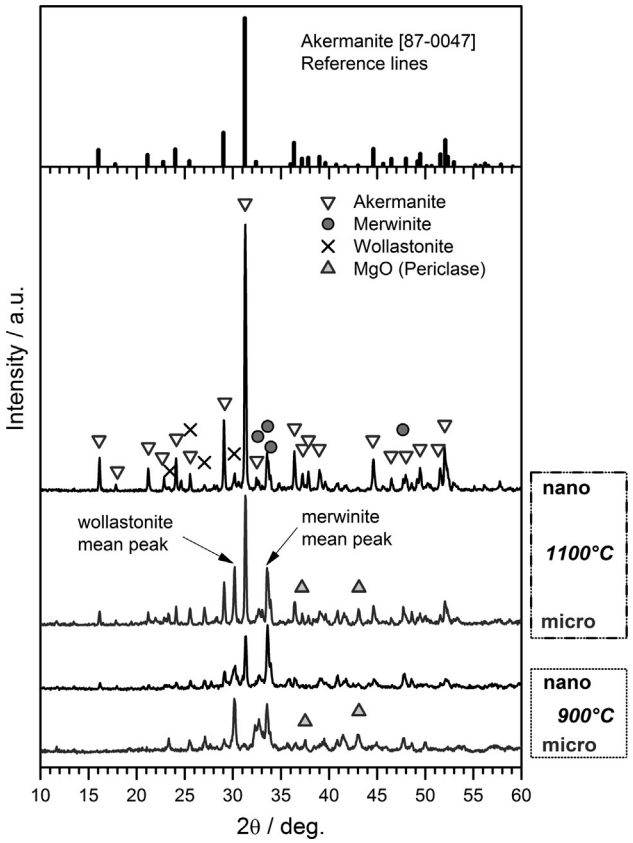

Fig. 1. Phase evolution of ceramics from silicone/fillers mixtures aimed at the synthesis of akermanite (micro = micro-sized fillers; nano = nano-sized fillers).

the best sample, obtained using nano-sized particles, was 85 wt% akermanite, 9% merwinite and 6% wollastonite. Since both wollastonite and merwinite are both bioactive [16], the presence of such impurities was not reputed to be an issue for the forecasted biological application of the material.

3.2. Development and characterization of akermanite-based ceramic composites

Hydroxyapatite (HAp) was introduced as additional filler in the best formulation for akermanite synthesis (the one comprising nano-sized fillers), in order to modify the biological response of the material and produce components possessing also a faster dissolution rate in biological fluids. Moreover, the addition of a further filler would potentially reduce the presence of cracks that were observed when processing the mixtures producing pure akermanite, despite the choice of a silicone mixture (MK+ H62C) as silica source, instead of only one silicone polymer. In fact, the use of a mixture of silicones has been proved to favor the integrity of polymer-derived silicates (a discussion of this effect has been recently provided by Parcianello et al. [15]), because the different chemical and structural characteristics of the polymeric precursors generate a silica matrix with different features (e.g. network connectivity and number of defects) which determine a different ability to relax structural rearrangements by viscous flow or diffusion processes.

HAp was added in several proportions (75 wt% CaO/MgO/SiO_2 ceramic residue from silicones and active fillers, 25 wt% HAp; 50–50 wt%, 25–75 wt%) and the samples were heat treated at 900 °C and 1100 °C. Only samples with 75% HAp were crack-free: the reduction of the transforming mass (silicone and active fillers) evidently reduced the stresses associated to the volumetric changes, in turn due to ceramic conversion and reactions giving the desired crystalline phases.

HAp, however, did not act simply as an inert filler: besides promoting the integrity of samples, it affected the phase development, as shown in Fig. 2, for samples containing 25% and 75% HAp. HAp peaks remained well recognizable for treatments at 900 °C, while at 1100 °C a novel phase formed, that is calcium phosphate silicate $Ca_5(PO_4)_2SiO_2$ (CPS, PDF♯40-0393), whose bioactivity was demonstrated only very recently [17]. Akermanite is clearly visible only for 25% HAp, at 1100 °C, whereas almost all samples contained merwinite. Some traces of unreacted MgO were detected for 25% HAp, at 900 °C.

Table 2 reports the results from mechanical testing of composites with 75% HAp fired at 1100 °C. The ceramic composites exhibited a sensible linear shrinkage (~15%) and were quite porous (~30 vol%), because of the production of decomposition gases during processing and limited solid state sintering at the processing temperature, with consequent limits on elastic modulus and strength. If we consider, however, that the composites could be applied in the form of scaffolds where all the constitutive elements are loaded as bars in bending configuration, we can note that the specific bending strength index is not far from that of important natural materials, such as cartilage (according to Ashby [18], $\sigma^{2/3}/\rho = 1.9$, where σ is the strength and ρ is the density). The specific bending stiffness index ($E^{1/2}/\rho$) was also close to that of natural materials. Improvements in strength could be obtained by coating the ceramic components with biopolymers [19], that could take advantage of the residual microporosity, clearly visible in Fig. 3a, for infiltration.

3.3. Development and characterization of akermanite ceramic foams

As previously reported, operating with H62C as the only silica source, the first drying step at 80 °C yields a thick paste. This condition has a great potential for further processing, since the high viscosity could promote the entrapment of gases. More precisely, $Mg(OH)_2$ and borax were considered for their ability to decompose at relatively low temperature, with a significant release of water vapor below 350 °C [20,21]. In other words, these fillers can be used for the double purpose of affecting the phase development and foaming.

The heating of the pastes at 350 °C was intended to: (i) provide the evolution of water vapor; (ii) stabilize the

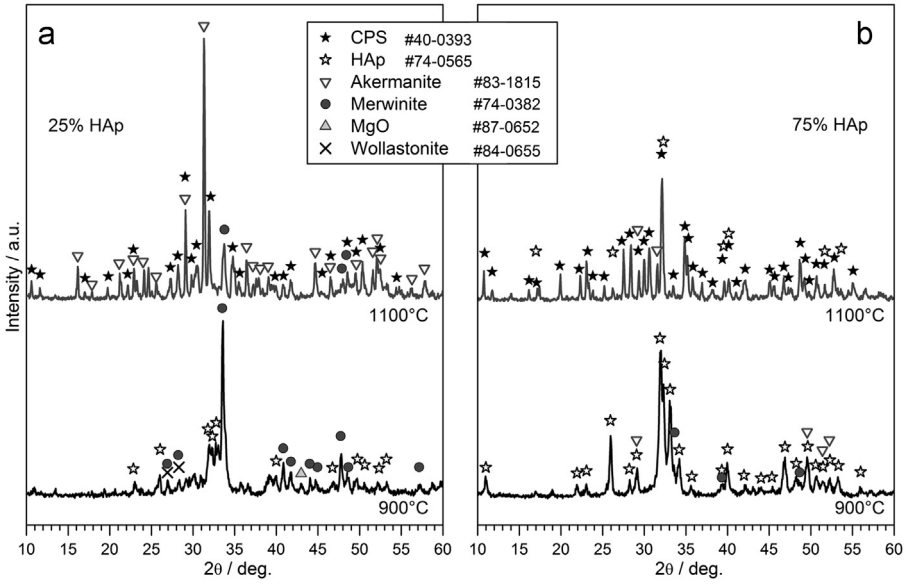

Fig. 2. Qualitative X-ray diffraction patters of akermanite-based ceramic composites, prepared with (a) 25% HAp; and (b) 75% HAp.

Table 2
Summary of physical and mechanical properties of selected akermanite-based bioceramics.

Type	Density, ρ (g/cm^3)	Total porosity (%)	Strength, σ (MPa)	Notes
25 Akermanite 75 HAp monolith (1100 °C)	2.53 ± 0.01	27	10.6 ± 1.5 (bending)	$E = 24.0 \pm 4.0$ GPa
Akermanite foams ($CaCO_3$ nano-particles)	0.86 ± 0.03	71	3.4 ± 0.2 (crushing)	No borax
	0.90 ± 0.02	69	5.1 ± 0.4 (crushing)	5% Borax
	0.85 ± 0.01	72	3.4 ± 0.4 (crushing)	15% Borax

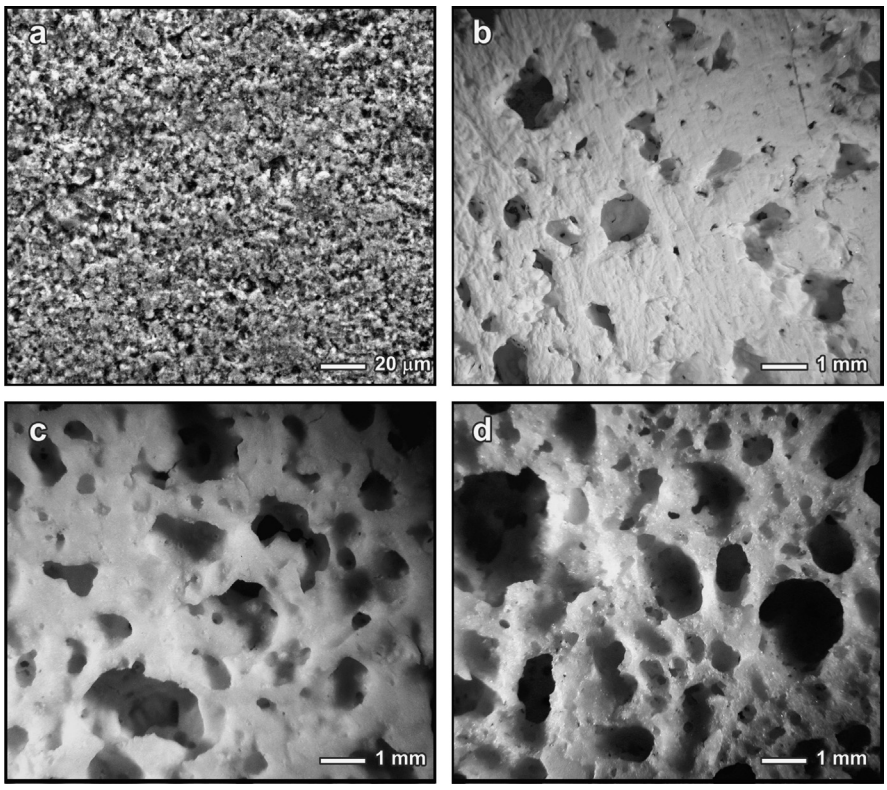

Fig. 3. Microstructural details of (a) akermanite/HAp ceramic composite (76% HAp); (b,c,d) akermanite based cellular materials (b) only $Mg(OH)_2$ as foaming agent; and (c) 5% borax; and d: 15% borax).

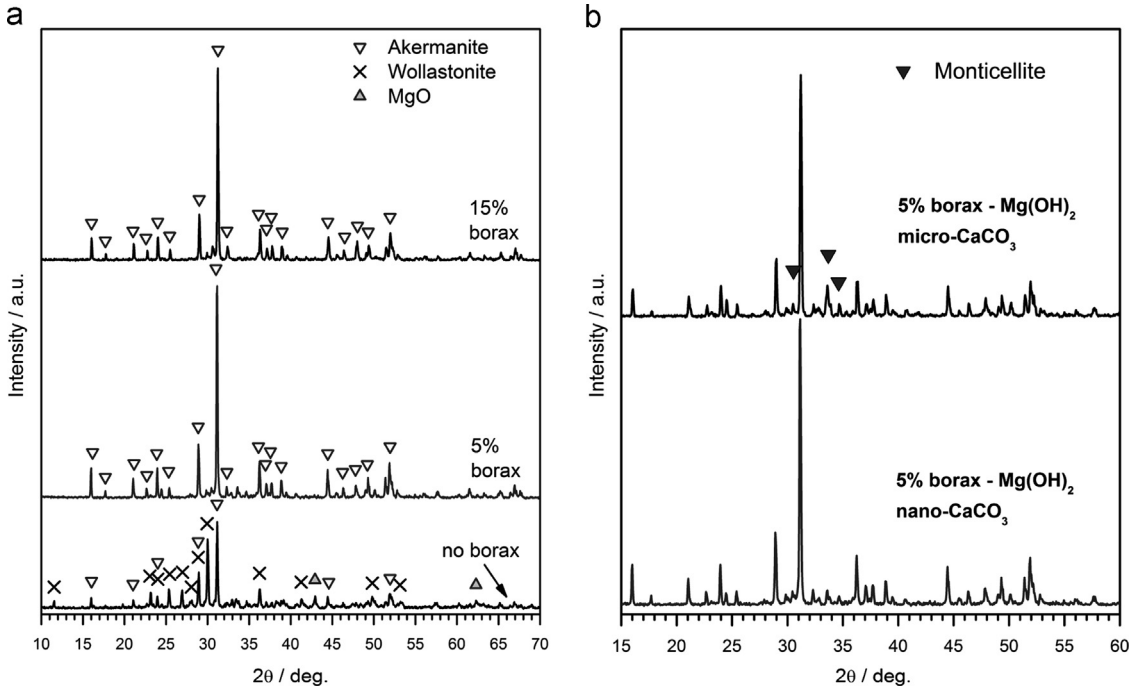

Fig. 4. X-ray diffraction patterns of akermanite foams (a) effect of borax and (b) effect of $CaCO_3$ powder size (not indexed peaks all corresponding to akermanite).

cellular structure by thermal cross-linking of the H62C polymer. As reported in Table 1, the sample resulting from the use of $Mg(OH)_2$ as the only water source was very porous (density well below 1 g/cm^3), but the pore distribution was not particularly homogeneous (see Fig. 3b). On the contrary, the addition of borax caused the formation of a well-developed cellular structure, with many clearly interconnected macro-pores (see Fig. 3c and d)

Borax had also a quite unexpected effect on the development of crystal phases. As shown by Fig. 4a, akermanite is not the only

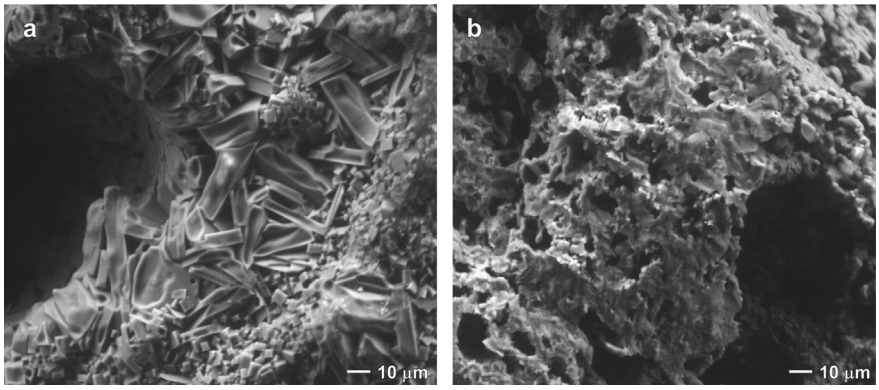

Fig. 5. High magnification details of akermanite foams (a) 15% borax and (b) 5% borax.

crystal phase that developed from mixtures comprising nano-sized $CaCO_3$ and micro-sized $Mg(OH)_2$: wollastonite and MgO (weak peaks) are also clearly visible. Mixtures comprising borax, on the contrary, featured only the presence of akermanite. We can posit that this additive led to the formation of a liquid phase upon ceramization (transformed into a borate glass phase upon cooling), thus favoring ionic interdiffusion. This is confirmed by Fig. 4b, showing that even operating only with micro-particles (micro-sized $CaCO_3$ replaced nano-sized $CaCO_3$) akermanite was the dominant phase (there are in fact only weak traces of a another Ca–Mg silicate, monticellite, $CaMgSiO_4$ i.e. $CaO \cdot MgO \cdot SiO_2$, PDF#35-0590).

Despite having a very similar bulk density, the crushing strength of the cellular ceramics (see Table 2) increased with the addition of a limited amount borax while, quite surprisingly, that was not observed for the sample with the most homogeneous porous structure (15% borax addition). A possible cause is the abnormal crystal growth of the silicate phase (embedded in a low viscosity borate phase), visible in Fig. 5a, leading to a number of microvoids. The abnormal crystal growth was not detected in the sample with a lower content of borax (5%), as shown in Fig. 5b.

The strength of the obtained foams, in all cases, compares favorably with the data reported in the literature for cellular akermanite (e.g. foams from conventional replication of PU templates possess a crushing strength well below 2 MPa [22]). The presence of B_2O_3 and Na_2O in the amorphous phase is not expected to compromise the bioactivity, since these oxides are present in bioglasses in much higher amounts [1]. The validation of the bioactivity and biocompatibility of the foams as well as the ceramic composites, will constitute the focus of future investigations.

4. Conclusions

The main findings of this study may be summarized as follows:

- Akermanite ceramics can be easily obtained by the thermal treatment of silicone resins embedding CaO and MgO precursors; the crystalline phase purity is optimized when adding nano-sized fillers.
- Hydroxyapatite powders, introduced as secondary fillers, interacted with the other components, leading to monolithic ceramic composites with complex phase assemblages and featuring a good specific strength; all the developed crystal phases are known to be biocompatible.
- A particular combination of starting materials, such as H62C polymer, nano-sized $CaCO_3$ and micro-sized $Mg(OH)_2$, was found to yield highly porous ceramic components, by a very simple process (low temperature foaming, followed by ceramization at 1100 °C).
- The addition of borax had a double effect, i.e. it contributed both to the development of an homogeneous cellular morphology and to the phase evolution; for borax-containing mixtures the resulting ceramics feature akermanite as the main phase.
- The newly developed foams compare favorably with cellular akermanite bioceramics previously reported in the literature; the oxides associated to borax addition (B_2O_3 and Na_2O) are not reputed to degrade the biocompatibility, being present in well-established biomaterials, such as bioglasses.

Acknowledgments

The authors acknowledge the financial support of the Italy–Germany bilateral research program “Vigoni”.

References

[1] M.N. Rahaman, D.E. Day, B.S. Bal, Q. Fu, S.B. Jung, L.F. Bonewald, A. P. Tomsia, Bioactive glass in tissue engineering, Acta Biomaterialia 7 (2011) 2355–2373.
[2] T. Kokubo, S. Ito, Z. Huang, T. Hayashi, S. Sakka, T. Kitsugi, T. Yamamuro, Ca–P-rich layer formed on high-strength bioactive glass-ceramic A-W, Journal of Biomedical Materials Research 24 (1990) 331–343.
[3] P.N. De Aza, F. Guitian, S. De Aza, Bioactivity of wollastonite ceramics: in vitro evaluation, Scripta Metallurgica et Materialia 31 (1994) 1001–1005.
[4] P.N. De Aza, Z. Luklinska, M.R. Anseau, F. Guitian, S. De Aza, Morphological studies of pseudowollastonite for biomedical application, Journal of Microscopy 182 (1996) 24–31.
[5] Z. Gou, J. Chang, Synthesis and in vitro bioactivity of dicalcium silicate powders, Journal of the European Ceramic Society 24 (2004) 93–99.

[6] A. Hoppe, N.S. Güldal, A.R. Boccaccini, A review of the biological response to ionic dissolution products from bioactive glasses and glass-ceramics, Biomaterials 32 (2011) 2757–2774.
[7] P. Revell, E. Damien, X. Zhang, P. Evans, C. Howlett, The effect of magnesium ions on bone bonding to hydroxyapatite, Key Engineering Materials 254–256 (2004) 447–450.
[8] H. Sun, C. Wu, K. Dai, J. Chang, T. Tang, Proliferation and osteoblastic differentiation of human bone marrow-derived stromal cells on akermanite-bioactive ceramics, Biomaterials 27 (2006) 5651–5657.
[9] C. Wu, J. Chang, Degradation, bioactivity, and cytocompatibility of diopside, akermanite, and bredigite ceramics, Journal of Biomedical Materials Research Part B 83B (2007) 153–160.
[10] C. Wu, M. Zhang, D. Zhai, J. Yu, Y. Liu, H. Zhu, J. Chang, Containerless processing for preparation of akermanite bioceramic spheres with homogeneous structure, tailored bioactivity and degradation, Journal of Materials Chemistry B 1 (2013) 1019–1026.
[11] S. Ni, L. Chou, J. Chang, Preparation and characterization of forsterite (Mg_2SiO_4) bioceramics, Ceramics International 33 (2007) 83–88.
[12] M. Kharaziha, M.H. Fathi, Synthesis and characterization of bioactive forsterite nanopowder, Ceramics International 35 (2009) 2449–2454.
[13] P. Colombo, E. Bernardo, G. Parcianello, Multifunctional advanced ceramics from preceramic polymers and nano-sized active fillers, Journal of the European Ceramic Society 33 (2013) 453–469.
[14] E. Bernardo, P. Colombo, E. Dainese, G. Lucchetta, P.F. Bariani, Novel 3D wollastonite-based scaffolds from preceramic polymers containing micro-and nano-sized reactive particles, Advanced Engineering Materials 14 (2012) 269–274.
[15] G. Parcianello, E. Bernardo, P. Colombo, Cordierite ceramics from silicone resins containing nano-sized oxide particle fillers, Ceramics International, http://dx.doi.org/10.1016/j.ceramint.2013.04.083, 2013, in press.
[16] M. Hafezi-Ardakani, F. Moztarzadeh, M. Rabiee, A. Reza Talebi, Synthesis and characterization of nanocrystalline merwinite ($Ca_3Mg(SiO_4)_2$) via sol–gel method, Ceramics International 37 (2011) 175–180.
[17] H. Demirkiran, A. Mohandas, M. Dohi, A. Fuentes, K. Nguyen, P. Aswath, Bioactivity and mineralization of hydroxyapatite with bioglass as sintering aid and bioceramics with $Na_3Ca_6(PO_4)_5$ and $Ca_5(PO_4)_2SiO_4$ in a silicate matrix, Materials Science and Engineering C 30 (2010) 263–272.
[18] M.F. Ashby, Materials Selection in Mechanical Design, Butterworth-Heinemann, Oxford, UK, 2005.
[19] K. Rezwan, Q.Z. Chen, J.J. Blaker, A.R. Boccaccini, Biodegradable and bioactive porous polymer/inorganic composite scaffolds for bone tissue engineering, Biomaterials 27 (2006) 3413–3431.
[20] I. Halikia, P. Neou-Syngouna, D. Kolitsa, Isothermal kinetic analysis of the thermal decomposition of magnesium hydroxide using thermogravimetric data, Thermochimica Acta 320 (1998) 75–88.
[21] I. Waclawska, Thermal decomposition of borax, Journal of Thermal Analysis 43 (1995) 261–269.
[22] C. Wu, J. Chang, W. Zhai, S. Ni, J. Wang, Porous akermanite scaffolds for bone tissue engineering: preparation, characterization, and in vitro studies, Journal of Biomedical Materials Research 76A (2006) 76–80.